Nigerian Research Journal of Chemical Sciences **(ISSN: 2682-6054)**
Volume 11, Issue 1, 2023

ADSORPTION OF CADMIUM IONS (Cd^{2+}) FROM AQUEOUS SOLUTION BY SUGAR CANE BAGASSE ACTIVATED CARBON -Fe_3O_4 MAGNETICNANO-COMPOSITE: KINETICS AND ISOTHERMS STUDIES

*Abdullahi Muhammad, Auwal Yushau and Kamaluddeen Suleiman Kabo

Department of Chemistry, Federal University, Dutsin-Ma, Katsina, Nigeria

*Corresponding Author: abchemist2020@yahoo.com, amuhammad2@fudutsinma.edu.ng

ABSRACT

The current trend of environmental pollution most especially heavy metal contamination brought about by anthropogenic factors needs to be check-mated in order to save the lives and well-being of man and other organisms as well as the environment. Achieving this aim requires the use of cheap materials and processed via green technology. Biomass has fulfilled these criteria of being bio-degradable, low-cost and efficient. Sugar cane bagasse activated carbon was chosen for this study and modified to form magnetic nanocomposite (SBAC/Fe_3O_4) as a way of improving its efficiency for adsorption of Cd^{2+} ions in aqueous medium. It was characterized by FT-IR, SEM and UV-Visible spectroscopy. Batch adsorption method was used to evaluate parameters such as pH at zero point charge, adsorbent dosage and initial concentration. The equilibrium experimental data fitted both Langmuir and Freundlich adsorption isotherms. The Langmuir adsorption capacity was 17.182 mg/g. Kinetics studies revealed the adsorption mechanism, reaction pathways and the solute uptake. Pseudo second order kinetics with R^2 value of 0.983 was found to be followed.

Keywords: Activated carbon, Biomass, Cadmium(II) ions, Langmuir, Magnetic nanocomposite, Sugar cane bagasse.

INTRODUCTION

Water contamination with different pollutants (mainly heavy metals and dyes) has become a major environmental problem and a threat to the well-being of living organisms [1-3]. Heavy metals are non-biodegradable, persistent and toxic in nature and are widely distributed in the environment [4]. They bioaccumulate in living organisms, through the food chains, thereby, causing different diseases and malfunctioning of organs [5].

Cadmium, chromium and copper are among few heavy metals that are discharged from several industrial effluents [1]. Cadmium is liberated into the environment from steel production, cement manufacture, Ni-Cd battery manufacture, cadmium electroplating, phosphate fertilizers [1, 4].

It has a maximum permissible limit of 0.003 ppm in drinking water going by the guidelines of World Health Organization (WHO) [6]. Zaini *et al* [7] reported that bivalent cadmium causes several deformities in humans such as muscular cramps, pulmonary problems, renal degradation, proteinuria, skeletal deformity and testicular atrophy.

In view of health concerns and environmental challenges associated with the consumption of food, drinking water and air, there is a compelling need to come up with a cheap method of adsorbing this heavy metal to ensure fulfillment of national safety guidelines on food, drinking water and our environment when industrial wastes are discharged into the environment [8]. Therefore, safeguarding public health and the environment must be done through compliance with drinking water and Industrial waste standards.

Activated carbon is widely used in various processes as an inexpensive and effective adsorbent [9, 10]. It is usually prepared from organic matter that contains of highly carbonaceous materials. Making agricultural wastes an interesting choice because of its low cost and it is a source of renewable energy [7]. The precursor material is chosen from critical examination of its percentage by dry weight of carbon (C), hydrogen (H), nitrogen (N) and sulphur (S) [1, 7, 10]. Sawdust [11], apricot stone [12], pecan shell [13], corncob [14] and coconut shell [15] were among the various carbon rich material wastes that have been used to produce activated carbon. Chemical activating agents that produced a larger surface area and high yield are H_3PO_4, H_2SO_4, $ZnCl_2$, NaOH and KOH. Zinc chloride ($ZnCl_2$) reported the highest yield [7]. Activated carbon is not the only base material used for adsorption. Other adsorbents include natural fibers, carbon nanotubes, zeolites, polymeric materials and magnetic nanocomposite [3, 16, 17].

However, new challenges in the development of novel materials as adsorbent still exist for proper effluent treatment [1]. In the present study, sugarcane bagasse was used in the preparation of activated carbon before modifying it to produce magnetic nanocomposite. Fe_3O_4 was chosen because of its unique characteristics of less toxicity, high efficiency and easy separation from aqueous medium [3].

This paper investigated the ability and efficiency of the prepared nanocomposite in removing Cd^{2+} from aqueous solution, by evaluating the effects of parameters such as pH, adsorbent dose, contact time and initial concentration of Cd^{2+} ions. Kinetic and isotherm parameters of the process were also among other things characterized.

MATERIALS AND METHODS

Chemicals and Reagents

All the chemicals and reagents used were analar and were purchased from Sigma Aldrich Inc., USA.

Sample Collection

The biomass (sugarcane bagasse) was obtained from Dutsin-Ma local market, selected, washed with deionized water and dried under shed for three days before reducing it to powder.

Preparation of Sugar Cane Bagasse Activated Carbon

Exactly 200 g of the sugar bagasse powder was accurately weighed and impregnated in 200 g/dm^3 aqueous $ZnCl_2$ and left at room temperature to stand for 24 hours. Thereafter it was filtered, dried and calcined 400 °C for 2 hours [18].

Synthesis o of Iron oxide/Activated Carbon magnetic nanocomposite (Fe_3O_4/AC)

Magnetic Activated carbon nanocomposite (MAC) was synthesized by the incipient wetness impregnation method [10, 18-19]. Briefly, 30 g of activated carbon (AC) was added into a 300 mL solution containing $FeCl_2 \cdot 4H_2O$ (6 g) and $FeCl_3 \cdot 6H_2O$ (17 g), and was mixed gently with a mechanical stirrer (VWR, USA) in a round bottom flask. The solution was deoxygenated by purging with N_2 gas. After heating the solution to 80 ℃, 20 mL ammonium hydroxide (28-30%, Sigma-Aldrich Inc., USA) was added and further mixed for 20 min [20, 26]. The suspension was aged for 1 day at 25 ℃ and washed continuously with Milli-Q water and ethanol. The cleansed MAC samples were obtained from suspension with vacuum-filtration followed by freeze-drying (Labconco Co., MO, USA), which removed water and ethanol on surfaces and pores [19].

Characterization

The functional group, surface morphology and UV-Visible spectrophotometry of the synthesized adsorbents were conducted using Fourier transform infrared spectrometer (Bruker, USA, Alpha), SEM spectrometer (MODEL-PHENOM ProX) and Cary Series UV-visible spectrophotometer Agilent Technology.

Adsorption Experiments

Adsorption Kinetics

Adsorption kinetic experiments were conducted using 50 ppm Cd^{2+} ions at pH 6.0 and 1 g adsorbent at a stirring rate of 130 rpm. Suspensions were sampled in duplicate at 15 min interval till the equilibrium was attained. Absorption of each aliquot solution after filtering (0.22 µm) was measured by means of UV-visible spectrophotometer and was evaluated using different kinetic models. Accordingly, a control experiment was simultaneously run without the adsorbent. Similarly adsorption isotherms experiments were conducted at the same conditions [20].

The percentage removal of $Cd^{2+}$was calculated by the following equation:

$$Percentage\ removal\ Cd^{2+} = \frac{C_0 - C_e}{C_0} \times 100 \qquad (1)$$

$$Amount\ \ of\ Cd^{2+} adsorbed\ (q_e) = \frac{(C_0 - C_e)V}{m} \qquad (2)$$

Where C_o and C_e are initial and equilibrium concentrations of Cd^{2+} (mg/L) respectively, m is the mass of the adsorbent (g) and V is the volume of Cd^{2+} solution.

RESULTS AND DISCUSSION

Characterization of Adsorbent

Fourier Transform Infrared Spectroscopy

The FT-IR spectra of the adsorbents were obtained to determine the functional groups formed which may be responsible for the attachment of the Cd^{2+} ions. The FTIR spectra of chemically activated AC, magnetic nanoparticle, NP, and activated carbon magnetic nanocomposite, AC-NP sorption of Cadmium Cd^{2+}ions were used to determine the vibrational frequency changes of the functional groups in the adsorbents. The spectra of adsorbents were measured within the range of 650–4000 cm^{-1} wave numbers. The spectra were plotted using the same scale on the transmittance axis for all the adsorbents before.

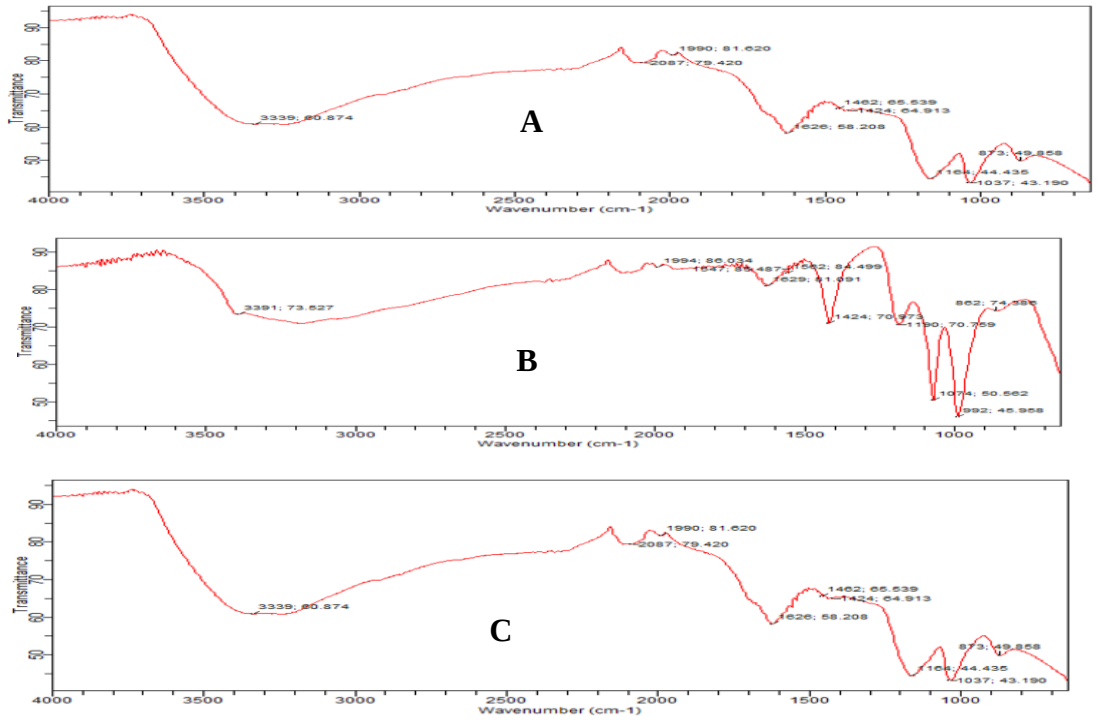

Figure 1: FT-IR Analysis of (A) Activated carbon, (B) Magnetic nanoparticle and (C) Activated carbon/Fe_3O_4 magnetic nanocomposite.

The FTIR spectra of the adsorbents displayed numbers of adsorption peaks, indicating the complex nature of the studied adsorbents. The peak at 873cm^{-1} is due to vibration of Fe-O confirming the incorporation of F_3O_4 into the activated carbon [3].

Table 1: Some fundamental infrared frequencies of the studied adsorbent

Adsorbents	Bonds Position cm^{-1}			
	O –H	C – H	C=O	C≡C
AC	3339	1462	1037	1626
NP	3391	1424	992	1629
AC–NP	3398	2880	1037	1626

UV-Visible Spectroscopy

Ultraviolet visible spectroscopy (UV-Vis) simply means an absorption spectroscopy or reference spectroscopy in the ultraviolet-visible spectral region. It involves the measurement of light

passing through a sample (*l*) and the intensities of the lights before and after passing through the sample is compared. The absorbance, A is related to the transmittance, T: A= -log (T).

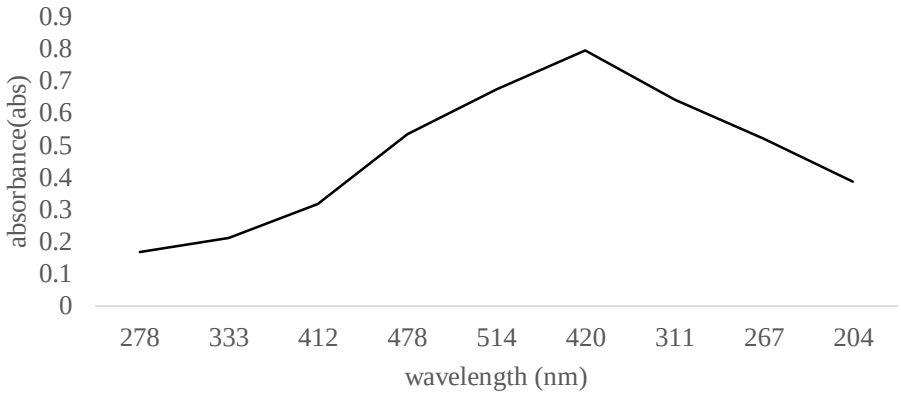

Figure 2: UV-Visible spectrum of AC–NP (Activated Carbon with Nanoparticle)

From Figure 2 which is the UV-Visible spectrum, it can be observed that the λ_{max} is 420 nm signaling the formation of nano-sized material [21].

Scanning Electron Microscopy

Surface morphology of NP (Nanoparticles), AC and AC-NP was visualized using Scanning Electron Microscopy (SEM). Measurements were taken using SEM-Quanta. The images were taken with an emission current of 100 μÅ by the Tungsten filament at a magnification of 750x and an accelerator voltage of 15 kV.

Figure 3 shows the SEM micrographs of AC (sugarcane bagasse activated carbon), Fe_3O_4 (Nanoparticles) and AC–NP. The AC exhibits homogeneous rough, dense and uneven surface morphology with a series of overlaps as shown. AC–NP shows the parent AC covered with Fe_3O_4 (NP), making a hybrid surface of moderately smooth and porous; thereby enhancing adsorption as well as particle diffusivity [22].

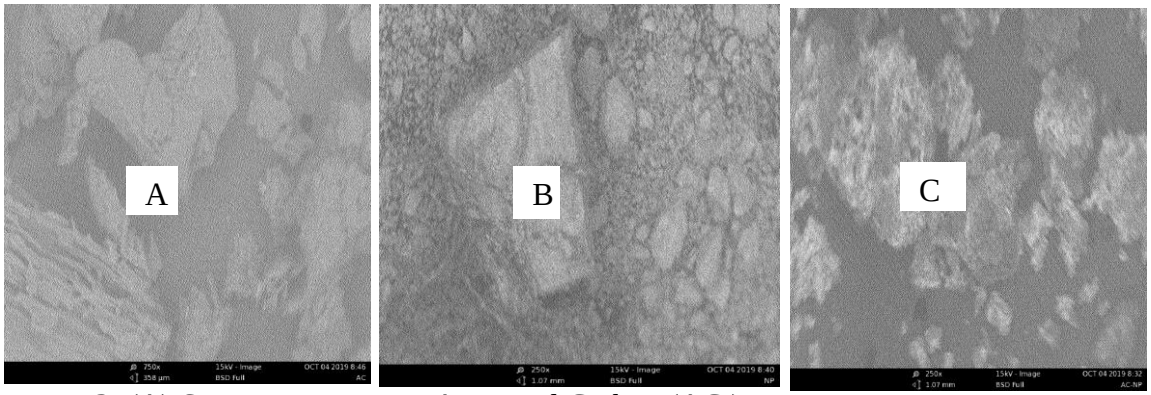

Figure 3: (A) Sugarcane Bagasse Activated Carbon (AC),
(B) Fe_3O_4 nanoparticles (C) Sugar Cane Bagasse Activated Carbon Coated with Nanoparticle (AC-NP).

Batch adsorption studies

Batch equilibrium studies

pH point at zero charge (pHpzc)

The pH for which the surface of the composite bears a zero net charge was determined by using 0.1mol/L NaCl solution. The initial pH of these solutions was maintained in the range of 1-12 by means of 0.1M HCl and NaOH. About 0.1 g of the adsorbent was added into each container and agitated for 48 h at 25 ^{0}C. It was then filtered and the final pH of the residual solution was taken. pHzpc is the point at which the initial and the final pH of NaCl were equal [20, 22].

The result showed that pHzpc of the SCB/Fe_3O_4 magnetic nanocomposite is 6.7. Hence the surface of the adsorbent bears a negative charge at pH>6.7 and positive at pH<6.7. Adsorption efficiency of the adsorbent increased from pH 3 to 10 with significant increase in alkaline media (pH>pHzpc). The interaction can be as a result of strong gravitational force and decrease of repulsive force between the adsorbent surface and Cd^{2+} ions [24]. The decrease in adsorption efficiency in acidic medium is due to competition of adsorbate with H^+ ions on the active sites of the adsorbent [24, 25].

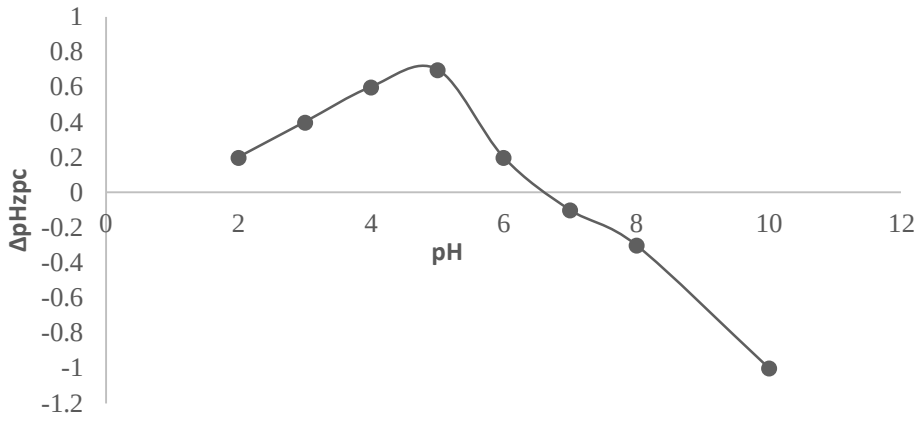

Figure 4: pH at zero point charge.

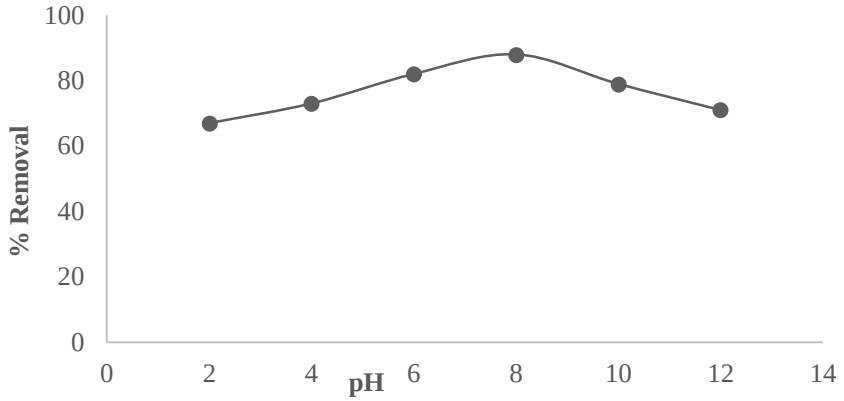

Figure 5: pH Effect

Effect of Adsorbent Dosage

The optimum amount of the adsorbent was investigated by varying its dosage from 0.1 to 0.5 g in 50 mL of 100 ppm of Cd^{2+} ions solution at 150 rpm while keeping all other parameters constant in accordance with optimization method based on one factor at a time [20, 26]. From the results showed in Figure 6, highest percentage removal of the metal ions is 92% at 0.3 g beyond which was a plateau. It may be due to the saturation/equilibrium of the active sites on the adsorbent surface or decline in the surface area caused by the agglomeration of the adsorbent [27].

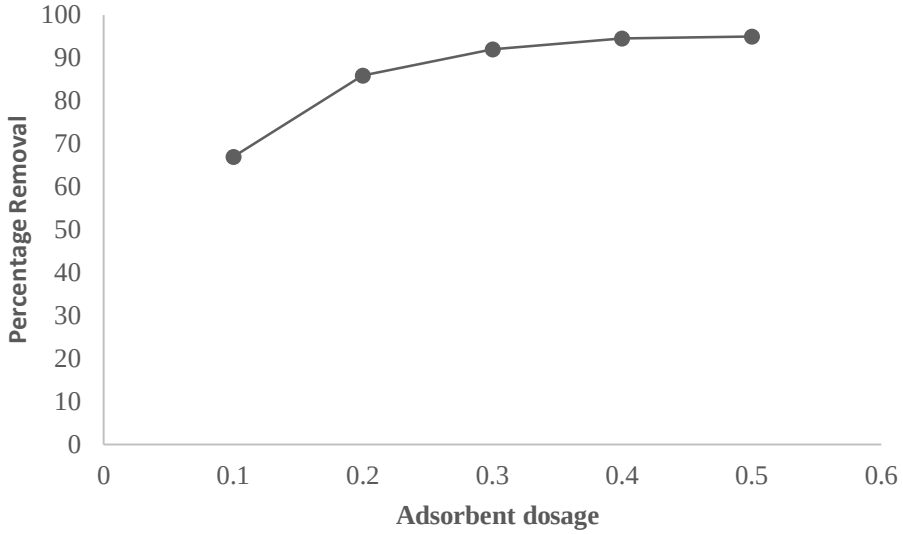

Figure 6: Effect of adsorbent dosage

The effect of initial concentration

Here the aim is to find the concentration of the adsorbate at which the adsorbent will have the maximum percentage removal. Therefore, the initial concentration of the adsorbate was ranged from 150 to 350 ppm and subjected to adsorption procedure while other factors are the same. From one 150 ppm to 300 ppm there was an increase in the adsorption which is due to low adsorbate/adsorbent ratio. The sharp decrease which follows later is due saturation of the sites as a result of increase in the ratio [27].

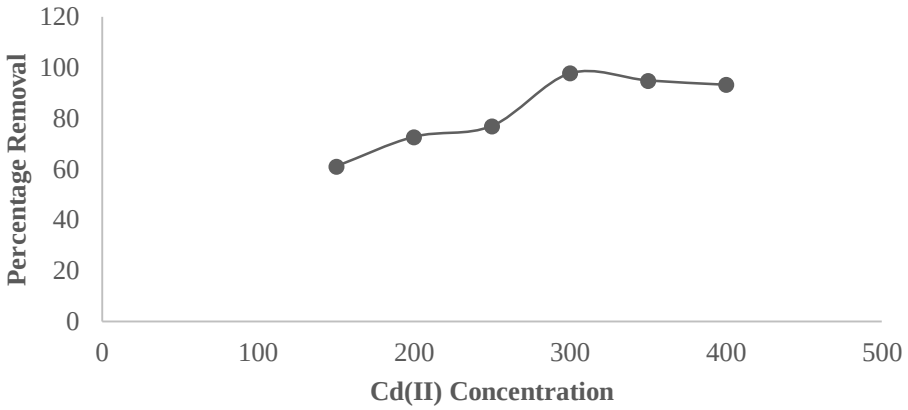

Figure 7: Effect of initial adsorbate concentration

Adsorption Isotherm

Batch adsorption data was described using Langmuir and Freundlich models for the evaluation of adsorption capacities. The Langmuir isotherm model is based on the assumption that monolayer adsorption occurs at homogeneous active sites in the adsorbent structure; while the Freundlich model is based on the assumption that adsorption occurs at heterogeneous and non-uniform surfaces [3, 26] and that all the binding sites have equal affinity for the adsorbate [28].

Langmuir Isotherm

The linearized model of Langmuir adsorption is stated below in equation (3).

$$\frac{C_e}{q_e} = \frac{1}{K_l q_m} + \frac{C_e}{q_m} \quad \text{.....(3)}$$

Where, C_e is the equilibrium concentration of the adsorbate (mgL^{-1}), qe is the amount of adsorbate adsorbed per unit mass of the adsorbent (mg/g), q_m and K_l is the Langmuir constants related to adsorption capacity and energy of adsorption.

The values of qm and K_l were determined from slope and intercepts of the plot and are presented in Table 2 respectively. The more the R^2 value fitted the Langmuir for the fact that it approaches unity [9]. A plot of Ce/qe against Ce as shown in figure 8, gave a straight line with a slope of $1/q_m$ which clearly indicates conformity to the Langmuir isotherm.

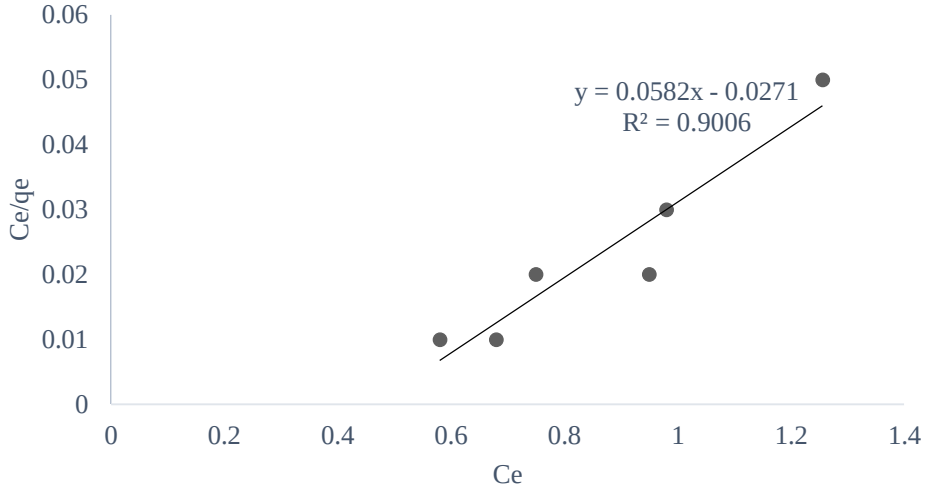

Figure 8: Langmuir Isotherm plot for removal Cd (II) ion on SBAC/Fe_3O_4.

Freundlich Isotherm

For the Freundlich isotherm, the values of *1/n*= 0.979 and n=1.02 fitting experimental data R^2=0.9252 indicate that both the physical process and the normal Langmuir isotherm are favourable.

$$\log q_e = \log K_f + \frac{1}{n}\log C_e \quad \text{.....(4)}$$

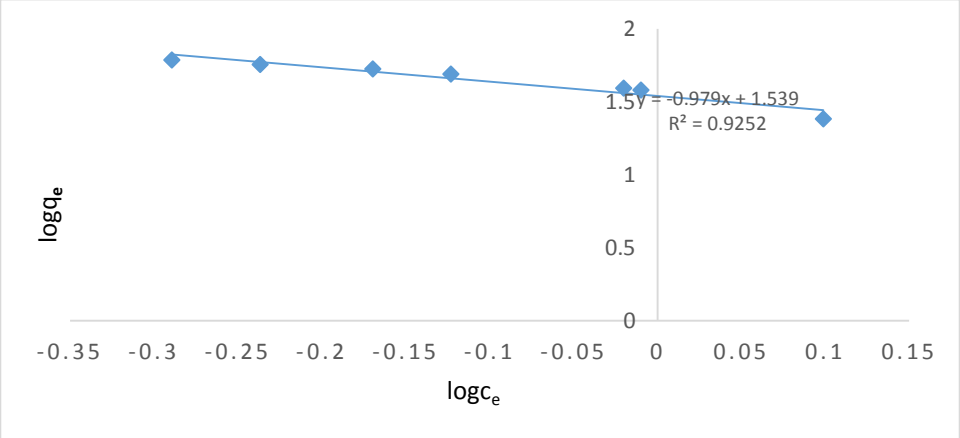

Figure 9: Freundlich Isotherm plot for removal Cd(II) on SBAC/Fe_3O_4.

Table 2: Comparison of Adsorption Isotherm Parameters of SBAC-Fe_3O_4 Nanocomposite

Langmuir Isotherm			Freundlich Isotherm		
q_m (mgg^{-1})	k_l(mgL^{-1})	R^2	k_f (mgg^{-1})	1/n	R^2
17.182	2.1476	0.9006	34.59	-1.021	0.9252

Adsorption Kinetics

The adsorption kinetics depends on the chemical and physical characteristics of the adsorbent. It describes the rate of the reaction and reaction pathways as well [29]. These kinetics models are pseudo-first order, pseudo-second order and intra-particle diffusion model. The adsorption in solid–liquid system was described by Pseudo-first-order kinetic model.

Pseudo First Order Model

The linear form of pseudo first order kinetic model, proposed by Lagergren is given in equation [30]:

$$\frac{dq_t}{dt} = k_1(q_e - q_t) \quad \text{.....(5)}$$

Where, q_e is the amount of metal adsorbed at equilibrium (mg g^{-1}), $q_t$is the amount of dye adsorbed at time "t" (mg g^{-1}), k_1 is the first order rate constant (min^{-1}) and t is the time (min).

Definite Integration of equation (5) within the boundary of t = 0 to t = t and qt = 0 to $q_t = q_e$ gives equation

$$\log(q_e - q_t) = \log q_e - \frac{k_1}{2.303} t \quad \text{.....(6)}$$

The linear graph of log(q_t- q_e)against t was plotted from the experimental data and used to find k_1 and R^2.

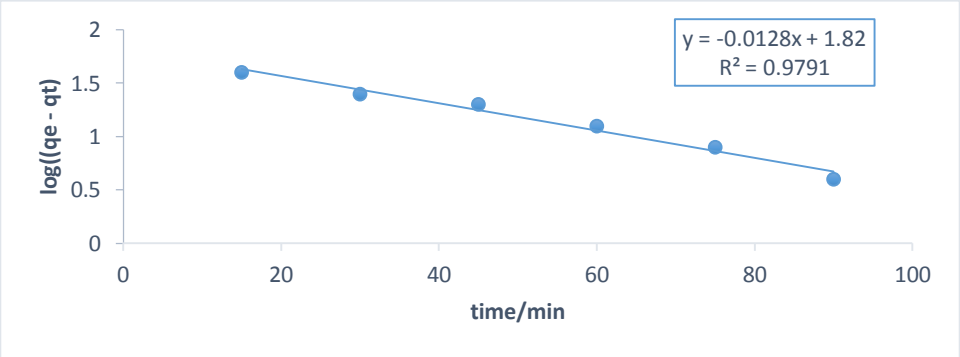

Figure 10: Pseudo First Order Kinetic Model Plot for the Adsorption of Cd(II) by SBAC-Fe_3O_4 nanocomposite.

Pseudo Second Order Model

Ho [31] developed another model to describe the kinetics of adsorption with the expressed as:

$$\frac{dq_t}{dt} = k_2(q_e - q_t)^2 \quad \text{.....(7)}$$

Where k_2 is the second order rate constant (g/mg min^{-1}).

Definite Integration of equation (7) within the boundary of t = 0 to t = t and $q_t = 0$ to $q_t = q_e$ gives equation (8) which the expression for the integrated linearized form of the pseudo second order kinetic model.

$$\frac{t}{q_t} = \frac{1}{k_2 q_e^2} + \frac{1}{q_e} t \quad \ldots\ldots\ldots\ldots\ldots\ldots\ldots (8)$$

Linear relationship was established in a plot of t/q_t versus t if the adsorption process obeys the pseudo second order kinetic model.

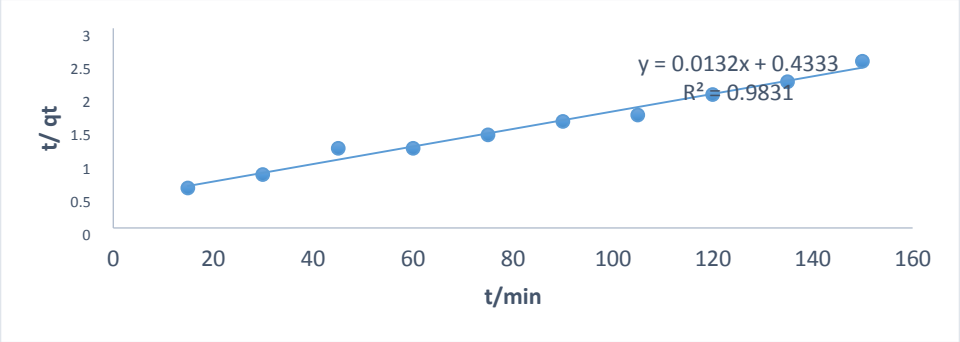

Figure11**:** Pseudo Second Order Kinetic Model Plot for the Adsorption of Cd(II)ionsby SBAC-Fe_3O_4.

Table 3: Comparison of Kinetic Parameters for the Adsorption of Cd^{2+} ions by SBAC- Fe_3O_4

Pseudo First Order			Pseudo Second Order		
q_e (mgg^{-1})	k_1 (min^{-1})	R^2	q_e (mgg^{-1})	k_2(g^{-1}mg min)	R^2
66.07	0.0295	0.9791	75.7576	0.0004	0.9831

Comparison of Adsorption Capacities

In order to fully appreciate the achievement of the current study, a comparison of its adsorption capacity with other reported in the literature have been shown in Table 4.

Table 4: Comparison of SBAC/Fe_3O_4 magnetic nanocomposite adsorption capacity with other adsorbents used in treating adsorbate

Adsorbent	Adsorption Capacity	Adsorbate	Reference
AC/Chitosan composite	52.63 mg/g	Cr(IV) and Cd(II)	[1]
ACL/Fe_3O_4magnetic	35.31 mg/g	Crystal Violet Dye	[3]
CNT/MgO/$CuFe_2O_4$	36.46 mg/g	Cationic dyes	[8]
PPAC	370.86 mg/g	(RBBR) dye	[9]
Fe_3O_4/Fish scale	68.72 mg/g	Methylene blue	[26]
GSAC/Fe3O4	50.51 mg/g	Methylene blue	[27]
SBAC/Fe_3O_4)	17.18 mg/g	Cd(II)	This study

CONCLUSION

Sugar bagasse activated carbon/Fe_3O_4 magnetic nanocomposite was synthesized by chemical precipitation and used as an adsorbent for the study of adsorption of cadmium (II) ions in aqueous solution. It shows a higher percentage adsorption at low initial concentration of the adsorbate and a pH_{zpc} of 6.7. Adsorption kinetics of Cd(II) ions using the adsorbent were tested using pseudo-first order and pseudo-second order kinetics models. The adsorption process followed pseudo-second order kinetics revealing that it is controlled by chemisorption. From the equilibrium data, Langmuir adsorption isotherm was best fitted indicating monolayer adsorption of Cd(II) ions onto the sugar cane bagasse activated carbon magnetic nanocomposite from aqueous solution with the adsorption capacity of 17.18 mg/g. Therefore, SBAC/Fe_3O_4 is a good potential, low cost and effective adsorbent for Cd(II) ions from aqueous solution.

REFERENCES

[1] Hakimeh, S., Mahboubeh, N. & Mansooreh, S. (2016). Evaluation of adsorption efficiency of activated carbon/chitosan composite for removal of Cr(VI) and Cd(II) from single and bi-solute dilute solution. *Advances in Environmental Technology,* 4,215-227.

[2] Gupta, V. K., Agarwal, S. & Saleh, T. A. (2011). Synthesis and characterization of alumina-coated carbon nanotubes and their application for lead removal. *Journal of hazardous materials,* 185(1), 17-23.

[3] Rauf, F., Seyed, J. P., Seyed H. P., Mirian, P. & Jose, M. L. (2021). Adsorption of crystal violet dye using Activated Carbon of Lemon Wood and Activated Carbon/Fe_3O_4Magnetic nanocomposite from aqueous solution: a kinetic, equilibrium and thermodynamic study. *Molecules, 26,2241.https://doi.org/10.3390/molecules26082241.*

[4] Mahfuza, S., Sultana, S.,Rana, S.,Yamazaki, T. A. & Yoshida, S. (2017). Health risk assessment for carcinogenic and non-carcinogenic heavy metal exposures from vegetables and fruits of Bangladesh. *Cogent Environmental Science,* 3, 1,1291107.

[5] Abdullahi, A., Lawal, M. A. & Salisu, A. M. (2021).Heavy metals in contaminated soil: source, accumulation, health risk and remediation process. *Bayero Journal of Pure and Applied Sciences,* 14(1),1-12.

[6] WHO (2013). Tech. Rep., "Guidelines for the safe use of waste water and food stuff". Report of the joint WHO/FAO Volume 2 No. 1, World Health Organization (WHO) and Foodand Agriculture Organization (FAO), Geneva, Switzerland, 2013.

[7] Muhammad, A. A. Z, Reiko, O. & Motoi, M. (2009). Adsorption of aqueous metal ions on cattle- manure- compost based activated carbons. *Journal of Hazardous Materials,* 170(2-3), 1119-1124.

[8] Foroutan, R., Peighambardoust, S. J., Esvandi, Z., Khatooni, H. & Ramavandi, B. (2021). Evaluation of two cationic dyes removal from aqueous environment using CNT/MgO/$CuFe_2O_4$ magnetic composite powder: a comparative study. *J. Environ. Chem. Eng.* 9(2), 104752.

[9] Mohd, A. A., Nur, A.A. P. & Olugbenga, S. B. (2014). Kinetic, equilibrium and Thermodynamic studies of synthetic dye removal using pomegranate peel activated carbon prepared by microwave induced KOH activation. Water *Resources and Industry, http://dx.doi.org/10.1016/j.wri.2014.06.002.*

[10] Zoha, H., Mohammad, H. D., Mohsen, H., Gholamali, J.,Imran, A. & Mika, S. (2020) Methods for preparation and activation of activated carbon: a review. *EnvironChemLett, DOI: 10.1007/s10311-019-00955-0.*

[11] Kalavathy, M. H., Karthikeyan, T., Rajgopal, S. & Miranda, L.R. (2005), Kinetic and isotherm studies of Cu(II) adsorption onto H_3PO_4-activated rubber wood sawdust. *J. Colloid Interface Sci.* 292(2),354–362.

[12] Khan, M.N. & Wahab, M. F. (2007). Characterization of chemically modified corncobs and its application in the removal of metal ions from aqueous solution, *J. Hazard.Mater.* 141(1), 237–244.

[13] Kobya, M., Demirbas, E., Senturk, E. & Ince, M. A. (2005). Adsorption of heavy metal ions from aqueous solutions by activated carbon prepared from apricot stone, *Bioresour. Technol.* 96, 1518–1521.

[14] Yahya, M.A., Al-Qodah, Z. & Ngah, C. Z. (2015). Agricultural bio-waste materials as Potential sustainable precursors used for activated carbon production: a review. *Renew Sustain Energy Rev*, 46,218–235. https://doi.org/10.1016/j.rser.2015.02.051.

[15] Sekar, M.V. & Sakthi, S. R. (2004). Kinetics and equilibrium adsorption study of lead(II) onto activated carbon prepared from coconut shell.*J. Colloid Interface Sci., 279,307–31.*

[16] Zhao, Z., Bai, C.,An, L., Zhang, X., Wang, F., Huang, Y., Qu, M. & Yu, Y.(2021). Biocompatible porous boron nitride nano/microrods with ultrafast selective adsorption for dyes. *J. Environ. Chem. Eng.*, 9, 104797.

[17] Bharatraj, S. R., Narendra, P. S. C., Perumal, P., Sapana, J., Mahmood, B., Suresh, C. A. & Rakshit, A. (2022). Synthesis and characterization of Ch-PANI-Fe_2O_3 nanocomposite and its water remediation applications. *Water*, 14, 3615.

[18] Spagnoli, A. A, Giannakoudakis, D. A. & Bashkova, S (2017). Adsorption of methylene blue on cashew nut shell based carbons activated with zinc chloride: the role of surface and structural parameters.
J.Mol Liq, 229,465–471. *https://doi.org/10.1016/j.molliq.2016.12.106*.

[19] Zhihui, D., Wanhui, Z., Muwen, L., Zhiwei, S., Weilin, H., Jing, L., Yanan, L., Juncheng, M., Yongtao, L. & Chengyu, C.(2020). Magnetic Fe_3O_4/activated carbon for combined adsorption and Fenton oxidation of 4-chlorophenol.*Carbon,(15375)doi: https://doi.org/10.1016/j.carbon.2020.05.106.*

[20] Panneerselvam P., Norhashimah, M., Kah, A. T. (2010). Magnetic nanoparticle (Fe_3O_4) impregnated onto tea waste for the removal of nickel(II) from aqueous solution. *Journal of Hazardous Materials*, 186,160–168.

[21] Abbas, Q. *(*2019). Understanding the UV-Vis spectroscopy for nanoparticles. *J NanomaterMolNanotechnol*, 8(3), 1-3. *doi: 10.4172/2324-8777.1000268.*

[22] Shehu, A., Ibrahim, M. B. & Umar, M. T. (2022). Aqueous phase adsorption of dyes onto activated carbon prepared from *Vitellaria paradoxa*(Shea Butter) Leaves: kinetic and thermodynamic Studies. *ChemSearch Journal*, 13(2),62–71.

[23] Hakimeh, S., Mahboubeh, N. & Mansooreh, S. (2016). Evaluation of adsorption efficiency of activated carbon/chitosan composite for removal of Cr(VI) and Cd(II) from single and bi-solute dilute solution. *Advances in Environmental Technology*, 4,215-227.

[24] Saeed, A., Sharif, M. & Iqbal, M. (2010). Application potential of grapefruit peel as dye sorbent: kinetics, equilibrium and mechanism of crystal violet adsorption. *J. Hazard. Mater.*,*179*, 564–572.

[25] Sakin, O. O., Hussein, M.A., Hussein, B. H. M. & Mgaidi, A. (2018). Adsorption thermodynamics of cationic dyes (methylene blue and crystal violet) to a natural clay mineral from aqueous solution between 293.15 and 323.15 K. *Arab. J. Chem.*, *11*, 615–623.

[26] Sharma, Y.C. & Srivastava, V. (2010). Separation of Ni(II) ions from aqueous solutions by magnetic nanoparticles. *J. Chem. Eng. Data*, 55, 1441–1442.

[27] Nima, G. A., Ahmad, D. K. & Azadeh, E. P. (2018). Fabrication, characterization, regeneration and application of nanomagneic Fe_3O_4@Fish scale as a bio-adsorbent for removal of Methylene Blue. *J. Water Environ. Nanotechnol.*,3(3), 219-234.

[28] Imam, S. S. & Abdullahi, M. (2017). Adsorptive removal of methylene blue using groundnut shell activated carbon coated with Fe_2O_3. *IOSR Journal of Applied Chemistry (IOSR-JAC)*,10(4),12-21.

[29] Chetan, S. U., Atharva, N. T., Jotiram, G. G. & Shriram, S. S. (2022). Low-cost adsorbents and nanomaterials for removal of heavy metals from contaminated water: review. *Journal of Indian Association for Environmental Management*, 42(4), 1-9.

[30] Huang, Y., Zeng, X., Guo, L., Lan, J., Zhang, L. & Cao, D. (2018). Heavy metal ion removal of wastewater by zeolite-imidazolate frameworks. *Sep. Purif. Technol.*194,462–469.

[31] Vikal, G., Jaya, A., Manisha, P., & Veena, (2007). Adsorption studies of Cu(II) from aqueous medium by Tamarind Kernal Powder. *Res. J.Chem. Environ.*,11(1), 40-43.